Scaling laws of femtosecond laser pulse induced breakdown in oxide films

M. Mero, J. Liu,* and W. Rudolph[†]

Department of Physics and Astronomy, University of New Mexico, Albuquerque, New Mexico, 87131, USA

D. Ristau and K. Starke

Laser Zentrum Hannover e.V., D-30419, Hannover, Germany

(Received 23 July 2004; revised manuscript received 21 October 2004; published 15 March 2005)

The scaling of the single-pulse laser threshold fluence for dielectric breakdown with respect to pulse duration and material band gap energy was investigated in the subpicosecond pulse regime using oxide films (TiO_2, Ta_2O_5, HfO_2, Al_2O_3, and SiO_2). A phenomenological model attributes the pulse duration dependence to the interplay of multiphoton ionization, impact ionization, and subpicosecond electron decay out of the conduction band. The observed linear scaling of the breakdown fluence with band gap energy can be explained within the framework of this model by invoking the band gap dependence of the multiphoton absorption coefficient from Keldysh photoionization theory. The power exponent κ of the observed dependence of the breakdown threshold fluence F_{th} on pulse duration τ_p, $F_{th} \propto \tau_p^{\kappa}$, is independent of the material and is attributed to photoionization seeded avalanche ionization.

I. INTRODUCTION

Femtosecond laser-induced breakdown of dielectric materials has gained a great deal of attention.[1] From a fundamental science point of view the phenomenon is interesting because it involves matter in a state far from thermal equilibrium whose behavior is governed by complex interactions between electrons, ions, and photons. The interest in applied science, in particular in high-precision micromachining, stems from the more deterministic nature of the breakdown and ablation threshold compared to picosecond and nanosecond pulses, allowing for smaller and cleaner structures.[2–5] Moreover, laser damage of optical components imposes severe constraints on the design and the materials used in the development of subpicosecond laser systems delivering energies approaching the kilojoule level.

Numerous experimental studies dealt with the dependence of the critical pulse fluence F_{th} on the pulse duration τ_p,[2,6–9] the laser wavelength λ,[2,5,10,11] and the material.[2,5,6,8,10,11] These experiments were conducted on fluorides, oxides, and glasses using near infrared and visible laser pulses with durations as short as a few femtoseconds.

The actual processes leading to femtosecond laser-pulse-induced dielectric breakdown and ablation are complex and still under investigation. Proposed mechanisms for material breakdown and removal include Coulomb explosion,[12] thermal melting (heterogeneous and homogeneous nucleation),[12,13] plasma formation,[13] and material cracking due to thermoelastic stresses.[14] Common to all these scenarios is that a critical amount of energy density has to be deposited in the material before breakdown occurs. In the subpicosecond pulse regime the absorption of near IR photons in dielectrics leads to the excitation of electrons to the conduction band (CB). Models that identify the onset of damage with the production of a certain critical CB electron density N_{cr} were suggested early on[15] and proved successful in explaining the observed $F_{th}(\tau_p)$ behavior until today.[2,6,7,9]

Two mechanisms can contribute to the generation of CB electrons—photoionization and electron impact ionization, the latter of which can result in an exponential increase of the number of excited electrons (avalanche ionization). For pulses longer than a few 10 ps, the applicability of the avalanche ionization model to intrinsic, bulk, single-shot laser damage was refuted based on experimental evidence[16] and theoretical calculations[17] for the case of a band gap energy and photon energy ratio of $E_g/(\hbar\omega) < 5$. In the ultrafast pulse domain, the relative contribution of the two effects and their dependence on material and pulse parameters are still debated. (See, e.g., Refs. 2, 18, and 19.) To explain the dependence of the breakdown threshold fluence on pulse duration, using the critical electron density as damage criterion, photoionization seeded avalanche was invoked.[2,6,7,9] In contrast, measurements of the intensity-dependent carrier density and the relaxation rates of high-energy CB electrons were interpreted as a result of a negligible contribution of impact ionization compared to photoionization.[19]

Most of the dielectric breakdown studies with femtosecond laser pulses were performed on bulk materials. The goal of our contribution is to characterize the pulse duration and band gap dependence of the damage threshold of oxide films experimentally and theoretically. Such films are widely used for optical coatings. Our results show that in the highest-quality films available today the subpicosecond damage behavior is controlled by intrinsic material properties rather than the impurities and defects introduced in the coating process and that the breakdown thresholds approach that of bulk materials. This is unlike what was observed previously with nanosecond pulses.[20] Breakdown measurements on thin films avoid problems arising from self-focusing in bulk materials, but interference effects have to be taken into account in the data analysis. Using five different films (TiO_2, Ta_2O_5, HfO_2, Al_2O_3, and SiO_2) manufactured under identical conditions we were able to explore the effect of the band gap energy E_g on the breakdown behavior. Using a phenomenological model based on the critical electron density concept,[2,15] we

TABLE I. Sample parameters. n_0, index of refraction at $\lambda = 800$ nm; D, film thickness; E_g, band gap energy.

Material	n_0	D (nm)	E_g (eV)
TiO$_2$	2.39	496	3.3
Ta$_2$O$_5$	2.17	546	3.8
HfO$_2$	2.09	568	5.1
Al$_2$O$_3$	1.65	716	6.5
SiO$_2$	1.50	790	8.3

FIG. 1. Incident laser fluence at which dielectric breakdown occurs measured as a function of the pulse duration for five oxide films.

will identify three figures of merit that characterize subpicosecond optical damage and can guide future developments of damage resistant optical coatings. The analysis of the experimental $F_{th}(\tau_p)$ and $F_{th}(E_g)$ behavior suggests a simple phenomenological formula for $F_{th}(E_g, \tau_p)$ that is valid in a wide range of band gap energies and pulse durations. Various breakdown scenarios that are based on the critical electron density criterion are analyzed with respect to their ability to explain this functional form. Finally, the relative weight of impact ionization and photoionization is investigated based on the predictions of the rate equation model and our experimental data.

II. EXPERIMENT

Dielectric films made from five different oxides—TiO$_2$, Ta$_2$O$_5$, HfO$_2$, Al$_2$O$_3$, and SiO$_2$—with band gaps ranging from 3.3 to 8.3 eV were investigated, see Table I. The films were deposited on 6.35 mm fused silica substrates by ion-beam sputtering (IBS) with a physical thickness of $6\lambda/4n_0$, where n_0 is the refractive index of the material at the wavelength $\lambda = 800$ nm. In contrast to conventional thermal evaporation processes, which are mostly applied for optical coatings, IBS produces films with superior optical quality, damage resistance, extremely low defect density,[21] and a film structure that is dense and nearly amorphous. Single pulses at a center wavelength of 800 nm from a femtosecond Ti:sapphire oscillator-amplifier system were used to excite the samples.[9] The pulse fluence was varied with neutral glass filters and a pair of Brewster plates. The pulse duration was tuned from 25 fs to 1.3 ps by adjusting a prism compressor at the amplifier output and inserting glass slabs of various lengths into the beam path. The beam waist at the sample was $w_0 \approx 20~\mu m$. The increased surface scattering of the laser light at damaged sites is routinely exploited in damage detection.[21] In our experiment the occurrence of damage was monitored with a charge-coupled device (CCD) camera-microscope detector. This allowed us to monitor the intensity and distribution of light scattered at the excited sample site.[9] For illumination we used the (amplified) spontaneous emission (ASE) leaking through the amplifier. The energy contrast of amplified pulse and ASE was greater than 10^3. This together with the highly nonlinear character of the excitation excludes multiple pulse effects (incubation) caused by the ASE. In a separate set of experiments we checked the scattering technique by off-line optical microscopy. A distinct change of the scattered intensity (pattern) of the weak ampli-
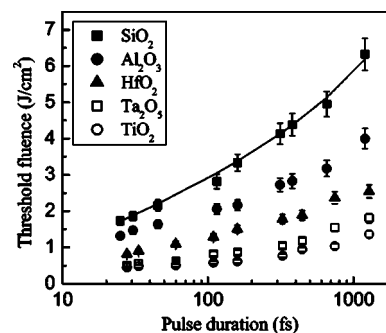
fied spontaneous emission was visible at the point of surface damage. The sample was translated after each pulse regardless of whether damage occurred to avoid incubation effects. The energy of each single excitation pulse, W, was measured and divided by the effective spot area to obtain the fluence $F = 2W/(\pi w_0^2)$. The knife-edge method was used to scan the focused (Gaussian) beam and determine the beam waist. After each shot the state of the illuminated site (0 for no damage, 1 for damage) and the corresponding fluence value were recorded and used to determine the damage probability curve. The 50% damage probability value was taken as the damage threshold. The reliability of damage detection using surface scattering was tested in a round-robin experiment, where it was demonstrated that single-pulse threshold fluences determined by different groups using both the scattering technique and Nomarski microscopy fall within a ±15% range if thick substrates are used.[21] It should be noted that the absolute threshold values are also affected by calibration errors of the energy detectors and uncertainties in the spot size measurements. Except for the shortest (bandwidth-limited) pulses, the measurements were performed with up-chirped pulses. Tests with down-chirped pulses did not result in different threshold fluences.

The measured damage fluences as a function of the pulse duration, $F_{th}(\tau_p)$, for the five oxide films are shown in Fig. 1. The threshold fluences refer to the incident fluences. The data analysis has to take into account interference effects inside the film, as the breakdown starts at the location of maximum intensity.[9] The maximum fluence in all of the films is about 0.7 times the incident fluence independent of the material. For all samples, two of the standing wave maxima are located at the air-coating and the coating-substrate interface. The threshold fluences were well defined and reproducible as indicated by the smallness of the error bars. This suggests that intrinsic material properties rather than stochastic defects and impurities introduced during the film deposition control the damage behavior. This conclusion is also supported by the fact that the threshold fluences are similar to those observed in bulk dielectric materials. See, for example, Refs. 7, 8, and 10.

III. MODELING

For many practical applications it is desirable to describe the damage behavior of optical materials with a simple

theory that requires only a few material parameters (figures of merit). Even though damage is a very complex phenomenon, the main excitation processes leading to dielectric breakdown in the subpicosecond pulse domain are often expressed in a rate equation for the electron density in the conduction band.[2,6,7,9,10] As will be shown below, in spite of its simplicity, this model can not only fit the experimental data, but it can also explain both the pulse duration and the band gap dependence of the breakdown threshold.

A complication in the modeling of the CB electron density is that not only excitation processes, but subpicosecond relaxation of electrons out of the conduction band also have to be taken into account. Such a relaxation was observed in bulk SiO_2, barium aluminum borosilicate,[22,23] and TiO_2, Ta_2O_5, and HfO_2 films,[24] and was interpreted as the formation of self-trapped excitons (STEs). Further evidence for STE formation in Ta_2O_5 films was obtained through fluorescence studies, which showed similarities to STE fluorescence in SiO_2.[25] We include this process by an effective relaxation time T. The associated decay term is to represent both the electrons leaving the conduction band and the possible ionization of STEs (re-excitation) by the still present laser pulse. The quality of the fit does not depend on the functional form of the decay law.

The rate of electron generation due to excitation and relaxation is written as

$$\frac{dN(t)}{dt} = \alpha N(t)\xi I(t) + \beta_m [\xi I(t)]^m - \frac{N(t)}{T}. \quad (1)$$

Here N is the electron density, $I(t)$ is the pulse intensity, α is the avalanche coefficient, β_m is the multiphoton absorption (MPA) coefficient of order m, T is an effective relaxation time, and $\xi \approx 0.66$ is the ratio of the maximum internal and the incident intensity.[9,26] The MPA coefficient represents nonlinear excitation from both the valence band and the laser-induced trap states. The breakdown threshold is assumed to be reached when $N(t_{max}) = N_{max} = N_{cr}$ which can happen during or at the end of the pulse.

A generally accepted choice for N_{cr} is the plasma critical density, where the plasma frequency of the generated carriers is equal to the laser frequency.[2,27] At this carrier density of $N_{cr} \approx 10^{21}$ cm^{-3} strong absorption of 800 nm laser radiation occurs. In the framework of this model, the damage behavior of the material is characterized by the parameters (figures of merit) α, β_m, and T.

There are experimental results that suggest a pulse duration dependent N_{cr}.[19] As currently it is not clear how the excited carriers lead to the destruction of the solid, the actual N_{cr} vs τ_p dependence is not known. In the calculations below, we will use a constant N_{cr} equal to the critical plasma density, but we will also examine the data from the point of view of a pulse duration dependent critical density.

Equation (1) without the decay term was derived from a Fokker-Planck equation that describes the electron dynamics in the conduction band.[2] It is applicable when the rate of Joule heating in the conduction band is much larger than the cooling rate due to electron-phonon scattering, and when the so-called flux-doubling approximation[28] is valid. The latter

TABLE II. Material parameters obtained from a fit of the model [Eq. (1)] to the experiment. The quantity m is the order of the multiphoton process needed to excite the material with photons at $\lambda = 800$ nm. Avalanche coefficient α (cm^2/J), MPA coefficient β_m (cm^{2m-3} fs^{m-1}/J^m), and effective decay constant T (fs). The last column shows the reduced effective mass obtained from Eq. (2) corresponding to the β_m^{fit} value, where m_0 is the rest electron mass.

Material	m	α	β_m^{fit}	T	m_r^{MPA}/m_0
TiO_2	3	34	1.5×10^{23}	120	27.0
Ta_2O_5	3	11	6.7×10^{24}	490	1.9
HfO_2	4	10	2.9×10^{25}	1050	1.6
Al_2O_3	5	12	2.3×10^{24}	220	5.4
SiO_2	6	8	9.9×10^{25}	220	2.2

means that every CB electron that reaches the critical energy of impact ionization will immediately excite a new valence electron, resulting in two electrons, both at the bottom of the conduction band. Applied to other published experimental $F_{th}(\tau_p)$ data for dielectric materials, the model based on Eq. (1) yields a dominant contribution of avalanche ionization to the CB electron density for pulse durations as short as a few tens of fs.[2,6,7,9] As a result, the predicted threshold fluences are only logarithmically sensitive to the numerical value of N_{cr}.

Some models question the applicability of the avalanche term in the rate equation for pulse durations below a few hundred fs, depending on the material and the photon energy.[18] We chose the rate equation approach to analyze the femtosecond breakdown behavior of our films and to support a phenomenological scaling law of the threshold fluence vs τ_p and E_g obtained from the experiment to be discussed later. Rate equations have been applied successfully to predict the pulse duration dependence of the breakdown threshold fluence in the ultrashort pulse domain.[2,6,7,9,27] We will discuss separately the avalanche process and its importance for the scaling laws.

Equation (1) was solved numerically for Gaussian input pulses with the requirement that $N_{max} = N_{cr}$. For each material a set of figures of merit (α, β_m, T) was determined that fits the data of Fig. 1 best. Table II summarizes the results. One representative example of a fit is shown in Fig. 2 for Al_2O_3 (solid line). For comparison we also show the predicted threshold behavior when the α and β_m values are the same but without considering the relaxation term (dashed curve). The agreement between the solid and the dashed line is excellent up to a pulse duration of approximately 200 fs in spite of the similarly short decay constant, $T = 220$ fs. This is a result of the dominant avalanche contribution, as most of the electrons are generated at the tail of the pulse. Likewise, if we fit the data for $\tau_p < 200$ fs without a decay term we underestimate F_{th} for longer pulses. For some of the samples a rough fit for the whole pulse duration range is possible without the decay term; however, without the decay term, the extracted fit parameters α and β_m depend on the pulse duration range used in the fit. Furthermore, the inclusion of the decay term always improves the fit. It should also be mentioned that a fit of the data with the MPA or the avalanche term alone is not successful.
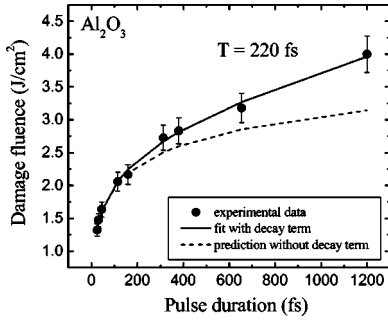
FIG. 2. Solid line: fit of the phenomenological model [Eq. (1)] with CB electron decay to the experimental data. Dashed line: prediction of threshold fluences using the same α and β_m values as in the case of the solid line, but without CB electron decay.

The values obtained for the avalanche coefficient agree well with the results of the numerical simulations in Ref. 2 and the fit results obtained in Ref. 6 for bulk fused silica. Depending on the material and excitation wavelength, MPA coefficients of a certain order can vary by several orders of magnitude (for β_3 values see, for example, Refs. 29 and 30). The coefficients determined by us through this indirect method are within these accepted ranges. For example, from Table II we get $\beta_3/\beta_6 \approx 10^{42}$ $(\mathrm{J/cm^2s})^3$, which is in agreement with what one expects from the literature.[31,32] This agreement also indicates that photoinduced defects have minor influence on the subpicosecond single-shot breakdown behavior.

The Keldysh theory of photoionization[33] provides an analytical formula for the MPA coefficient. For our sample parameters and the range of intensities involved in the experiments,

$$\beta_m \approx \frac{\omega}{9\pi}\left(\frac{m_r\omega}{\hbar}\right)^{3/2}\left(\frac{e^2}{8\omega^2 m_r c\varepsilon_0}\right)^m \frac{\exp(2m)}{(n_0 E_g)^m}, \qquad (2)$$

where ω is the carrier angular frequency of the laser pulse, $m = \mathrm{mod}(E_g/\hbar\omega)$ is the order of the multiphoton absorption process, m_r is the reduced mass, e is the electron charge, and c is the velocity of light in vacuum.

Strictly speaking, the MPA rate $\beta_m I^m$ with constant β_m and m is only applicable at low intensities and its use in Eq. (1) near breakdown field strengths is questionable. We therefore performed another fit where we replaced the MPA term in Eq. (1) with the exact Keldysh rate[33] and used (α, m_r, T) as free parameters. The so obtained values for α and T were essentially the same as those from the first fit. This was also true for the β values derived from Eq. (2) using the reduced mass from the second fit.

The reduced effective masses are not available in the literature for our films due to the unknown lattice and band structures. For bulk TiO_2, the CB electron effective mass varies from $20m_0$ for the rutile phase to m_0 for the anatase phase,[34] where m_0 is the rest electron mass. For bulk Ta_2O_5 and HfO_2, the CB electron effective mass is $0.1m_0$ and 0.3–$0.6m_0$, respectively.[35,36] For SiO_2, m_r is assumed to be in the range of 0.5–$1.0m_0$.[2,18] The reduced masses corresponding to the β_m fit values obtained using Eq. (2) are also shown

TABLE III. Values of κ in the scaling law $F_{th} \propto \tau_p^\kappa$ as a function of the investigated materials.

Material	E_g (eV)	κ
TiO_2	3.3	0.28 ± 0.02
Ta_2O_5	3.8	0.33 ± 0.02
HfO_2	5.1	0.30 ± 0.01
Al_2O_3	6.5	0.27 ± 0.01
SiO_2	8.3	0.33 ± 0.01

in Table II (last column). The values are in order-of-magnitude agreement with what one expects based on the bulk material properties.

The effective relaxation times extracted from the fit to the model range from 120 fs to 1 ps (Table II). As with the reduced masses, a comparison of T with literature data is difficult, if at all possible, because values for such time constants were observed in bulk materials. Electron relaxation and trapping times are known to be material-structure dependent and can be expected to vary significantly from thin films to bulk single crystals. For example, self-trapping of excitons was observed for anatase TiO_2, but not for rutile TiO_2.[34] The structural difference between our film materials and the corresponding bulk, crystalline materials also manifests itself as a difference in band gap energies, which for Al_2O_3, for example, can be as large as a few 10%. In addition, T as used in Eq. (1) is not a relaxation time in the usual meaning, as it includes effects of reexcitation. These differences in material structure could explain why a CB electron trapping time of ~ 100 ps was measured for crystalline Al_2O_3.[32]

IV. DISCUSSION

A double-logarithmic plot of the data of Fig. 1 (not shown) reveals straight lines for each material with a material independent slope of ≈ 0.3. In other words, $F_{th} = f(E_g)\tau_p^\kappa$ with $\kappa \approx 0.3$ independent of the band gap energy. Table III summarizes the actual values for κ for our five films obtained from a fit to the experiment. Similar power dependencies can be seen in multiple-shot experiments on bulk samples done by other groups.[2,6] The single-shot bulk breakdown thresholds in Refs. 7 and 8 also showed similar behavior albeit with a power coefficient $\kappa < 0.3$.

Figure 3 shows the measured breakdown fluences as a function of the material band gap energy for 30-fs and 1.2-ps pulse excitation. The same trend is obtained for the other pulse durations between 30 fs and 1.2 ps from the data presented in Fig. 1. The data sets were normalized to the fluence values observed in the material with $E_g = 5.1$ eV. One recognizes a linear behavior: $F_{th} = g(\tau_p) + h(\tau_p)E_g$. Within experimental error the normalized $F_{th}(E_g)$ curves for all pulse durations overlap, which suggests $g(\tau_p) = c_1 k(\tau_p)$ and $h(\tau_p) = c_2 k(\tau_p)$, where c_1 and c_2 are material and laser independent constants. The dashed line in Fig. 3 shows the common slope extrapolated to larger band gap values. It is interesting to note that data obtained by Stuart *et al.*[2] with different mate-
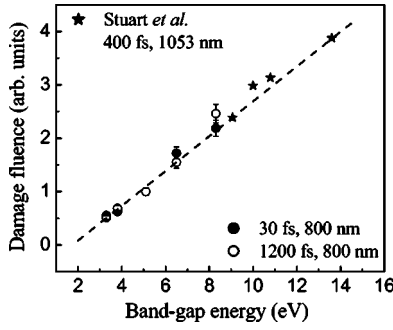
FIG. 3. Experimental breakdown fluence as a function of band gap energy obtained with 30 fs (solid circles) and 1.2 ps (open circles) laser pulses. The data points are normalized to the damage fluence at $E_g = 5.1$ eV. The data shown by asterisks were taken from Ref. 2.

rials (BaF$_2$, CaF$_2$, MgF$_2$, and LiF) and excitation conditions follow the same trend, cf. Fig. 3.

By comparison of the $F_{th}(\tau_p)$ and $F_{th}(E_g)$ dependencies we get $k(\tau_p) = \tau_p^\kappa$. Therefore, our experimental data suggest a scaling of the breakdown threshold fluence for the oxide films according to

$$F_{th}(E_g, \tau_p) = (c_1 + c_2 E_g)\tau_p^\kappa, \qquad (3)$$

with $c_1 = -0.16 \pm 0.02$ J cm^{-2} fs$^{-\kappa}$, $c_2 = 0.074$ ± 0.004 J cm^{-2} fs$^{-\kappa}$ eV^{-1}, and $\kappa = 0.30 \pm 0.03$ being material and pulse duration independent parameters. The error bars on c_1 and c_2 refer to the standard deviation of the best fit values obtained at different pulse durations. The error bar on κ is the uncertainty of the best fit values for the different materials. In contrast to the rate equation model, the only material parameter that enters the phenomenological formula expressed in Eq. (3) is the material band gap energy E_g. It remains to be seen if such a law also applies to other types of materials. The fact that the data by Stuart et al.[2] follow the same E_g dependence suggests that only a constant factor has to be included in Eq. (3), which depends on the material type and possibly on the specifics of the film deposition or material growth process. To obtain the critical incident fluence when dealing with thin films, Eq. (3) has to be divided by the correction factor ξ that takes into account interference effects.

In what follows, we will analyze Eq. (3) in the framework of the rate equation model with the critical CB electron density criterion.

Equation (1) with dominant avalanche ionization predicts a scaling $F_{th} \propto \tau_p^\kappa$ where κ is close to 0.3 in a large (α, β_m) parameter range. This is illustrated in Fig. 4 for excitation by six-photon absorption and impact ionization for pulse duration from 40 fs to 1.24 ps and a constant value of $T = 300$ fs. In the parameter range covered by Fig. 4, multiphoton absorption provides $\leq 1\%$ of the total CB electrons, with the highest value occurring at the shortest pulse duration in the simulation. In contrast, if we consider three-photon absorption combined with impact ionization, the maximum contribution of multiphoton absorption can be as large as a few 10% for $\tau_p = 40$ fs (not shown). It should be noted that
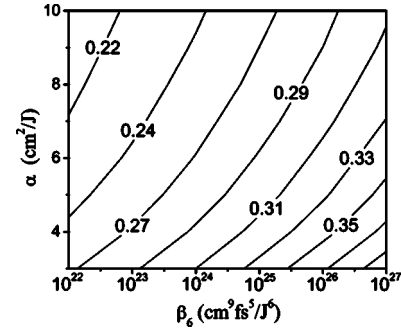

FIG. 4. Contour plot of the exponent κ as a function of the avalanche coefficient α and multiphoton absorption coefficient β_m for six-photon absorption and $T = 300$ fs.

different values for T produce qualitatively similar results. Therefore, the scaling of the breakdown threshold with pulse duration suggests that for large band gap materials photoionization provides only the seed electrons for the avalanche, while for low band gap materials it can have a contribution that is comparable to that of avalanche ionization for the shortest pulse durations. This supports the conclusions reached by others.[2,6,10]

Photoionization or avalanche ionization alone cannot explain that $F_{th} \propto \tau_p^\kappa$ with $\kappa \approx 0.3$. Pure photoionization in the multiphoton absorption limit produces $N \propto \int \beta_m I^m dt$ yielding $\kappa = (m-1)/m$, where the exponent varies with band gap energy. Thus $\kappa \geq 0.67$ is expected for our materials. The MPA term alone could reproduce the correct $F_{th}(\tau_p)$ dependence only with a strongly pulse duration dependent N_{cr}. To illustrate this point we calculate the ratio of electron densities produced by pulses of two different durations through multiphoton absorption only,

$$\frac{N_{\text{MPA}}(\tau_p)}{N_{\text{MPA}}(\tau_p')} = \left(\frac{F(\tau_p)}{F(\tau_p')}\right)^m \left(\frac{\tau_p'}{\tau_p}\right)^{m-1}. \qquad (4)$$

Using our experimentally measured fluence values for SiO$_2$ for example, the CB electron density at threshold should vary by more than three orders of magnitude when increasing τ_p from 80 fs to 1.2 ps. This factor of a few thousand is much larger than the experimentally determined factor of 20 by Quere et al. for SiO$_2$.[19] Using the full Keldysh photoionization formula[33] to take into account the interplay of tunneling and multiphoton absorption one obtains the following results. The log-log plot of F_{th} vs τ_p (not shown) consists of straight segments of slope $\kappa \approx (m-1)/m > 0.3$ separated by narrow regions of negative slope. The origin of these "steps" is the change of the effective band gap with intensity. The location of the steps depends on the effective mass. Numerical calculations based on the full Keldysh expression for SiO$_2$ predict that the CB electron density varies by a factor of a few hundred for $\tau_p = 80$–1200 fs, when the reduced effective mass is in the range of $m_{\text{red}} = 0.5$–$1.0 m_0$. If only avalanche ionization is present acting on background CB electrons from, for example, impurities, $\kappa = 0$ (Ref. 2).

To explain the nearly linear scaling of the threshold fluence with the band gap we proceed as follows. The processes for which an intrinsic E_g dependence can be expected are
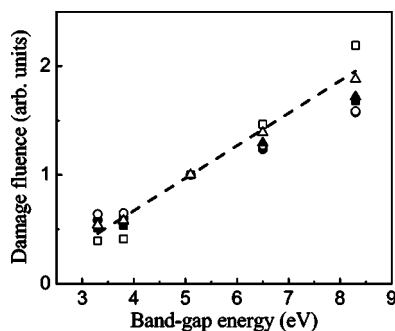
FIG. 5. Calculated breakdown fluence as a function of the band gap energy according to the model explained in the text. $\alpha=0$ (squares), $\alpha=10$ cm^2/J (circles), and $\alpha=14-9$ cm^2/J (triangles) in the range from 3.3 to 8.3 eV. The solid (open) symbols are for τ_p $=30$ fs (1200 fs). The data sets are normalized to the fluence values at 5.1 eV.

multiphoton absorption and impact ionization. The band gap dependence of β according to Keldysh theory is expressed in Eq. (2). The band gap dependence of impact ionization results from the fact that the CB electrons have to acquire an energy $E>E_g$ before an additional valence band electron can be promoted to the conduction band in a collision. This suggests a decreasing value of α, if the band gap increases.

Figure 5 illustrates the effect of the band gap dependence of β and α on the scaling of the threshold for 30-fs and 1.2-ps excitation pulses. The dashed line represents the trend line from Fig. 3 characterizing the experimental results. For the band gap dependence of the MPA coefficient, Eq. (2) is used with $m_r=0.5m_0$ and $T=1$ ps. Different values for T produce qualitatively similar results. To show that $F_{th}(E_g)$ is not sensitive to the band gap dependence of α, we plot three scenarios—(i) $\alpha=0$, (ii) $\alpha=10$ cm^2/J, and (iii) $\alpha=(30/E_g +5)$ cm^2/J, with E_g given in eV. The latter represents an avalanche coefficient that decreases from 14 to 9 cm^2/J, which roughly describes the results of the fit to the experiment. In all three cases the principal behavior of the experiment is reproduced; the simulated data fall into a narrow range about the trend line. An α that is monotonically decreasing with E_g leads to better agreement between experiment and theory than a constant α. Note that the slope of the experimental trend is also approximately reproduced. This

suggests that the major contributor to the band gap dependence of F_{th} is the multiphoton ionization process. It should also be noted that the slope of the quasilinear scaling of $F_{th}(E_g)$ is rather insensitive to the actual choice of the critical electron density within the reasonable limits of 10^{19} cm^{-3} $<N_e<10^{21}$ cm^{-3}.

V. SUMMARY

Laser breakdown thresholds as a function of pulse duration (25 fs–1.3 ps) and band gap energy (3.3–8.3 eV) of oxide dielectric films were measured. We found that the damage threshold is determined by intrinsic material properties rather than by the defects and impurities due to imperfections in the manufacturing process. The scaling of the threshold fluence with pulse duration is interpreted with a phenomenological rate equation model containing three material-dependent figures of merit; the multiphoton absorption coefficient, the impact ionization parameter, and an effective relaxation time of conduction band electrons. For each material the breakdown fluence scales as τ_p^κ, where $\kappa \approx 0.3$, and therefore is rather independent of the actual band gap energy. Based on the values of the fit parameters in the phenomenological model, we attribute this behavior to a dominant contribution of avalanche ionization to the carrier excitation even at pulse durations as short as a few 10 fs. As a result, the power law and the exponent κ are relatively insensitive to the actual values of the avalanche and multiphoton coefficients. The breakdown fluence at constant pulse duration shows an approximately linear dependence on the band gap energy. Photoionization was identified as the process that controls this behavior. These findings for the oxide films suggest a phenomenological formula $F_{th}=(c_1+c_2E_g)\tau_p^\kappa$, where the threshold fluence is determined by the band gap of the material only, with a possible additional factor that depends on the material type and growth process.

*Present address: Fudan University, Shanghai, China.

†Electronic address: wrudolph@unm.edu

[1] *Proceedings of the Laser-Induced Damage in Optical Materials, Collected papers, Boulder, 1999–2003*, edited by G. J. Exarhos, A. H. Guenther, N. Kaiser, M. R. Kozlowski, K. L. Lewis, M. J. Soileau, and C. J. Stolz (SPIE, Bellingham, WA, 2004).

[2] B. C. Stuart, M. D. Feit, S. Herman, A. M. Rubenchik, B. W. Shore, and M. D. Perry, Phys. Rev. B **53**, 1749 (1996).

[3] M. Lenzner, J. Krüger, W. Kautek, and F. Krausz, Appl. Phys. A: Mater. Sci. Process. **68**, 369 (1999).

[4] M. D. Perry, B. C. Stuart, P. S. Banks, M. D. Feit, V. Yanovsky,

and A. M. Rubenchik, J. Appl. Phys. **85**, 6803 (1999).

[5] A. P. Joglekar, H. Liu, G. J. Spooner, E. Meyhofer, G. Mourou, and A. J. Hunt, Appl. Phys. B: Lasers Opt. **77**, 25 (2003).

[6] M. Lenzner, J. Krüger, S. Sartania, Z. Cheng, Ch. Spielmann, G. Mourou, W. Kautek, and F. Krausz, Phys. Rev. Lett. **80**, 4076 (1998).

[7] A.-C. Tien, S. Backus, H. Kapteyn, M. Murnane, and G. Mourou, Phys. Rev. Lett. **82**, 3883 (1999).

[8] A. Rosenfeld, M. Lorenz, R. Stoian, and D. Ashkenasi, Appl. Phys. A: Mater. Sci. Process. **A69**, S373 (1999).

[9] J. Jasapara, A. V. V. Nampoothiri, W. Rudolph, D. Ristau, and K.

Starke, Phys. Rev. B **63**, 045117 (2001).

[10] C. B. Schaffer, A. Brodeur, and E. Mazur, Meas. Sci. Technol. **12**, 1784 (2001).

[11] D. M. Simanovskii, H. A. Schwettman, H. Lee, and A. J. Welch, Phys. Rev. Lett. **91**, 107601 (2003).

[12] R. Stoian, D. Ashkenasi, A. Rosenfeld, and E. E. B. Campbell, Phys. Rev. B **62**, 13 167 (2000).

[13] B. Rethfeld, K. Sokolowski-Tinten, D. von der Linde, and A. S. Anisimov, Appl. Phys. A: Mater. Sci. Process. **79**, 767 (2004).

[14] M. F. Koldunov, A. A. Manenkov, and I. L. Pokotilo, Quantum Electron. **32**, 335 (2002).

[15] E. Yablonovitch and N. Bloembergen, Phys. Rev. Lett. **29**, 907 (1972).

[16] S. C. Jones, P. Braunlich, R. T. Casper, and X.-A. Shen, Opt. Eng. **28**, 1039 (1989).

[17] D. Arnold and E. Cartier, Phys. Rev. B **46**, 15 102 (1992).

[18] A. Kaiser, B. Rethfeld, M. Vicanek, and G. Simon, Phys. Rev. B **61**, 11 437 (2000); B. Rethfeld, Phys. Rev. Lett. **92**, 187401 (2004).

[19] F. Quere, S. Guizard, Ph. Martin, G. Petite, H. Merdji, B. Carre, J.-F. Hergott, and L. Le Deroff, Phys. Rev. B **61**, 9883 (2000); F. Quere, S. Guizard, and Europhys. Lett. **56**, 138 (2001).

[20] T. W. Walker, A. H. Guenther, and P. E. Nielsen, IEEE J. Quantum Electron. **QE-17**, 2041 (1981).

[21] K. Starke, T. Groβ, and D. Ristau, in Proceedings of the Laser-Induced Damage in Optical Materials, Boulder 2000, [Proc. SPIE 4347, 528 (2001)]; J. Bonse, S. Baudach, J. Krüger, W. Kautek, K. Starke, T. Groβ, D. Ristau, W. Rudolph, J. Jasapara, and E. Welsch, [*ibid.* 4347, 24 (2001)].

[22] P. Martin, S. Guizard, Ph. Daguzan, G. Petite, P. D'Oliveira, P. Meynadier, and M. Perdrix, Phys. Rev. B **55**, 5799 (1997).

[23] M. Li, S. Menon, J. P. Nibarger, and G. N. Gibson, Phys. Rev. Lett. **82**, 2394 (1999).

[24] M. Mero, A. J. Sabbah, J. Zeller, and W. Rudolph, Appl. Phys. A (to be published); J. Zeller, A. J. Sabbah, M. Mero, P. A. Alsing, J. K. McIver, and W. Rudolph, in *Proceedings of the Laser-Induced Damage in Optical Materials, Boulder, 2003*, edited by G. J. Exarhos, A. H. Guenther, N. Kaiser, K. L. Lewis, M. J. Soileau, and C. J. Stolz (SPIE, Bellingham, WA, 2004), p. 515.

[25] M. Mero, B. Clapp, J. Jasapara, W. Rudolph, D. Ristau, K. Starke, J. Krüger, S. Martin, and W. Kautek, Opt. Eng. (to be published).

[26] J. Jasapara, M. Mero, and W. Rudolph, Appl. Phys. Lett. **80**, 2637 (2002).

[27] D. Du, X. Liu, G. Korn, J. Squier, and G. Mourou, Appl. Phys. Lett. **64**, 3071 (1994).

[28] M. Sparks, D. L. Mills, R. Warren, T. Holstein, A. A. Maradudin, L. J. Sham, E. Loh, Jr., and D. F. King, Phys. Rev. B **24**, 3519 (1981).

[29] M. I. Demchuk, V. S. Konevskii, N. V. Kuleshov, V. P. Mikhailov, P. V. Prokoshin, and K. V. Yumashev, Opt. Commun. **83**, 273 (1991).

[30] A. M. Streltsov, K. D. Moll, A. L. Gaeta, P. Kung, D. Walker, and M. Razeghi, Appl. Phys. Lett. **75**, 3778 (1999).

[31] R. W. Boyd, *Nonlinear Optics* (Academic Press, San Diego, 2003), p. 530.

[32] S. Guizard, P. Martin, Ph. Daguzan, and G. Petite, Europhys. Lett. **29**, 401 (1995).

[33] L. V. Keldysh, Sov. Phys. JETP **20**, 1307 (1965).

[34] H. Tang, K. Prasad, R. Sanjines, P. E. Schmid, and F. Levy, J. Appl. Phys. **75**, 2042 (1994).

[35] P. L. Young, J. Appl. Phys. **47**, 242 (1976).

[36] W. J. Zhu, T.-P. Ma, T. Tamagawa, J. Kim, and Y. Di, IEEE Electron Device Lett. **23**, 97 (2002).